ELSEVIER

Coordination Chemistry Reviews 237 (2003) 31–39

COORDINATION CHEMISTRY REVIEWS

www.elsevier.com/locate/ccr

Medium-dependence of vanadium K-edge X-ray absorption spectra with application to blood cells from phlebobranch tunicates

Patrick Frank [a,b], Robert M.K. Carlson [c], Elaine J. Carlson [d], Keith O. Hodgson [a,b,*]

[a] *Department of Chemistry, Stanford University, Stanford, CA 94305, USA*
[b] *Stanford Synchrotron Radiation Laboratory, SLAC, Stanford University, Stanford, CA 94309, USA*
[c] *Chevron Petroleum Technology Co., P.O. Box 1627, Richmond, CA 94802, USA*
[d] *Department of Biochemistry and Biophysics, University of California, San Francisco, CA 94143, USA*

Received 25 January 2002; accepted 23 August 2002

Contents

Abstract

K-edge X-ray absorption spectroscopy (XAS) is a subtle probe of the chemical environment and oxidation state of the elements. Thus, the change in the energy position of the rising K-edge inflection in the XAS spectrum of $[V(H_2O)_6]^{3+}$ in pH 0, 1, 2 and 3 aqueous solutions produces a titration curve that can be fit ($r = 0.999$) with an unusual model involving two cooperative deprotonations, yielding $pK_{a1} = 1.5 \pm 0.1$ and $pK_{a2} = 1.1 \pm 0.1$. These pH effects on V^{III} K-edge XAS spectra vary with the medium (40% aqueous methanol) and the counterion (Cl^-, SO_4^{2-}). Applied to whole blood of the tunicate *Ascidia ceratodes*, as collected from Monterey Bay, California, fits to the vanadium K-edge XAS spectra produced a detailed speciation of the major endogenous cellular V^{III} (complex, percent): $[V(H_2O)_6]^{3+}$, 23.6%; $[V(SO_4)(H_2O)_5]^{+}$, 38.1%; $[V(SO_4)_2(H_2O)_4]^{-}$, 19.8%, and; $[V(SO_4)(OH)_2(H_2O)_3]$, 7.7%. Genus-associated differences in the distribution of blood cell vanadium appear on comparison with a sample of whole blood from *Phallusia nigra*, in which most of the vanadium is distributed among $[V(H_2O)_6]^{3+}$, 34%; tris-chelated V^{III}, 33%, and; $[V^{IV}O(H_2O)_5]^{2+}$, 30%, with no V^{III} complex ions at all detected. Vanadium distribution in the blood cells of a single specimen of *A. ceratodes* from Bodega Bay, California is shown to vary significantly from the norm of animals collected from Monterey Bay, California. Finally, preliminary results are reported from in vitro experiments exposing *A. ceratodes* blood cells to vanadyl ion, showing active uptake and incorporation.

Keywords: Tunicate; Ascidian; Vanadium; X-ray; XAS; Speciation

1. Introduction

X-ray absorption spectroscopy (XAS) can be used to speciate elements of interest within complex regimes in terms of oxidation states and chemical environments [1–

* Corresponding author. Tel.: +1-650-926-3153; fax: +1-650-926-4100
E-mail address: hodgson@ssrl.slac.stanford.edu (K.O. Hodgson).

0010-8545/02/$ - see front matter © 2002 Elsevier Science B.V. All rights reserved.
PII: S0010-8545(02)00224-2

6]. In ascidian blood cells, vanadium [7,8] and sulfur [9,10] have been speciated, along with vanadium in tunichrome reaction products [11], using linear combinations of the XAS spectra of model complexes and solutions.

We present here recent results showing the effect of pH on the K-edge XAS spectrum of V^{III} in aqueous solution that exemplify the sensitivity of XAS spectroscopy to progressive changes in metal ligation. In addition, we summarize recent XAS modeling of vanadium in the blood cells of the two solitary tunicates, *Ascidia ceratodes* and *Phallusia nigra*, in terms of discrete inorganic complexes. Comparison is made between the environments of vanadium in the blood cells of *A. ceratodes* specimens collected from two disparate locations about 210 km apart along the central California coast. Finally, preliminary results are presented of experiments examining the in vitro uptake of vanadyl ion by, and fate within, *A. ceratodes* blood cells.

2. Materials and methods

Blood cell samples from *A. ceratodes* as collected from Monterey Bay, California or from Bodega Bay, California were prepared as described [7,12]. Likewise, preparation of blood cell samples from *P. nigra* collected from Key Largo, Florida, has been described [8,13]. In the incubation experiments, combined blood cells representing 14 *A. ceratodes* specimens collected from Bodega Bay, California was divided into three equivalent samples that were incubated concurrently for 40 min in an ice-bath. These samples included native blood cells used as a control, blood cells exposed to 25 mM dithiothreitol (DTT), and blood cells exposed to 25 mM each of added DTT and $VOSO_4$. The reagents were added as solutions in 0.5 M NaCl buffered to pH 6.6 with 25 mM sodium phosphate. After incubation, the cells were collected by centrifugation ($100 \times g$, 5 min), re-suspended in ice-cold 0.5 M NaCl in 25mM phosphate, pH 6.6, and centrifuged again. Finally, for XAS examination, a thick re-suspension of the blood cells was made in 0.5 M NaCl in 30% aqueous ethylene glycol [7,8]. This was introduced into a Lexan XAS sample cell and frozen in liquid nitrogen. Cell viability was confirmed by Trypan Blue exclusion assay, showing that the blood cells remained viable during this procedure. Trypan Blue solution was used as received (Sigma Chemicals).

A stock solution of 0.1 M VCl_3 in 1 M HCl, pH 0.0, was prepared by hydrogen reduction of solid V_2O_5 initially suspended in 1.3 M HCl with 100 mg of 10% Pd on C, as described [7]. The samples of VCl_3 in pH 1, 2, and 3 aqueous solution were prepared under a dinitrogen atmosphere in an inert atmosphere glove box (Plas-Labs, Lansing, MI). Appropriate aliquots of the stock 0.1 M VCl_3 solution were adjusted in pH using solid powdered KOH, with final pH values of 0.95, 2.06, and 3.07. Solution pH values were determined inside the glove box using an external Beckman 3500 pH meter connected to a combination pH electrode resident in the glove box and calibrated between pH 0.1 and 4.0. The XAS samples in Lexan sample cells were removed from the glove box and frozen immediately in a freezing *n*-pentane slush (−130 °C). The samples were stored in liquid nitrogen until XAS measurement. Samples of V^{III} in sulfuric acid solution of pH 0–3 were prepared from a stock solution of 0.5 M $V_2(SO_4)_3$ in 15 mM H_2SO_4 solution [14] using the same method. Samples of V^{III} in pH 0–3 in 40% aqueous methanol solution were prepared and measured as described previously [7].

The pK_a of bisulfate in 40% aqueous methanol was determined by triplicate titration of weighed samples of $NaHSO_4 \cdot H_2O$ (Baker Analyzed Reagent) dissolved in 25 ml of 40% methanol. The titration was carried out using 0.100 N NaOH made in 40% aqueous methanol by appropriate dilution of a 'Dilut-it' standard (Baker Analyzed Reagent). The titrations were followed using a Beckman model 3500 pH meter connected to a combination pH electrode that had been calibrated between pH 0.1 and 7.0. A correction of +0.1 pH unit was applied to the pH readings in order to refer them to water solution [15,16]. The pK_a of bisulfate in this medium was calculated from the reciprocal of the K_b, which was obtained by fitting the combined titration results with the equation for the protonation reaction: $K_b \times [H^+]_{free}/(1+K_b \times [H^+]_{free})$ [17]. The fit ($r = 0.997$), shown in Fig. 1, yielded a $pK_a = 2.45 \pm 0.01$.

XAS measurement of the blood cell samples of *A. ceratodes* from Monterey Bay, California [18], of those

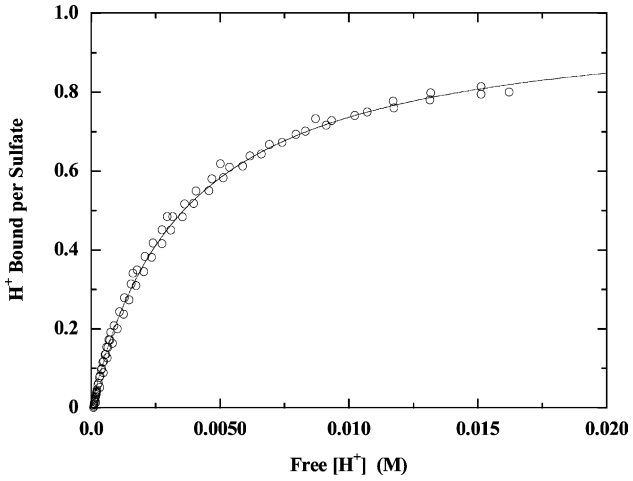

Fig. 1. Data from three titrations of bisulfate ion dissolved in 40% aqueous methanol. The line is the fit to the data according to the equation y = fraction of H^+ bound = $K_b \times [H^+]_{free}/(1+K_b \times [H^+]_{free})$ [17].

from Bodega Bay, California [12], and of *P. nigra* from Key Largo, Florida [8,13] have been described elsewhere. XAS spectra of 0.1 M VCl_3 in solutions of varying pH were measured on SSRL wiggler beamline 7-3 under dedicated operating conditions of 65–93 mA and a wiggler field of 17 kG. The X-ray beam was energy discriminated using a Si[220] double-crystal monochromator, detuned 50% at 5740 eV to minimize harmonic contamination. Vanadium K-edges were obtained as fluorescence–excitation spectra and measured by means of an Ar-filled fluorescence ionization detector (Stern–Heald–Lytle detector), set at 90° from the X-ray beam and equipped with a Ti filter and Soller slits. Samples of V^{III} in aqueous sulfuric acid of varying pH were likewise measured on wiggler beamline 7-3, at 64–91 mA and with an 18 kG wiggler field.

Vanadium foil calibrations were measured after every four scans, using an in-line nitrogen-filled ionization detector. All XAS samples were maintained at 10 K using an Oxford Instruments CF1208 continuous-flow liquid helium cryostat. Raw vanadium K-edge data were processed as has been described previously in detail [18,19]. The XAS data were calibrated to the first inflection on the rising edge of a vanadium foil standard, assigned to 5464.0 eV.

The equilibrium fit to the solution-state VCl_3 XAS data showing the shift with pH of the rising edge was carried out within the application Kaleidagraph, v3.5 (Synergy Software, Reading, PA) using the general curve-fitting routine which uses the Levenberg–Marquardt method [20]. The data to be fit were plotted as number of hydrogen ions bound per mole of V^{III} versus the concentration of free hydrogen ions in units of Molar, according to a model assuming sequential protonation of $[V(OH)_2(H_2O)_4]^+$. The function fit was $(K_{b1} \times [H^+]_{free} + 2 \times K_{b1} \times K_{b2} \times ([H^+]_{free})^2)/(1 + K_{b1} \times [H^+]_{free} + K_{b1} \times K_{b2} \times ([H^+]_{free})^2)$ [17,21]. K_{b1} and K_{b2} are the unknown first and second protonation constants, respectively, and '$[H^+]_{free}$' is the known concentration of free hydrogen ion, measured as pH and in units of Molar.

Calculation of the speciation of aqua-VCl_3 solutions across pH in terms of the hydrolytic vanadium complexes that are produced was carried out using the program Medusa v8.0, written by I. Piugdomenech, Department of Inorganic Chemistry, The Royal Institute of Technology, Stockholm, Sweden (http://www.inorg.kth.se). The various acidity and hydrolysis constants used in the speciation calculation were taken as appropriate from the set of results reflecting an ionic strength $\mu = 1.0$ M NaCl in the work of Meier et al. [22]. The vanadium speciation was calculated to reflect the concentrations used (0.1 M VCl_3; $\mu = 1.1$ in 1.0 M HCl, neglecting hydronium ion).

3. Results and discussion: vanadium K-edge XAS

In order to successfully speciate metals within a complex biological environment using XAS spectra, it is critical that the model solutions and complexes match as closely as possible the conditions found within the sample of interest. For that reason, a library of XAS spectra must be assembled covering the conditions known or hypothesized to exist within the sample. In application to the question of vanadium in the blood cells of phlebobranch tunicates, we have measured K-edge XAS spectra of vanadium in oxidation states III, IV, and V, and in a variety of solution and complexation environments. In these cases, the XAS spectra have proven to be very sensitive to variations in valence, in ligation-state, to the elemental identity of the complexing atoms, and to the symmetry of the ligation environment [7,8].

3.1. Response to solution pH

Thus in Fig. 2, the K-edge XAS spectra and the first derivatives of the XAS spectra of VCl_3 in aqueous solutions of pH 1, 2, and 3 are shown. Significant changes are observed in the rising edge region of the XAS spectrum, and at and above the energy of the absorption maximum at 5482 eV (Fig. 2a). Likewise, over the pH range 0.0–3.07, a progressive shift to lower energy totaling 2.0 eV was observed in the rising edge near 5480 eV (Fig. 2a, inset). These effects are more readily discerned in the first derivative spectra, Fig. 2b. Here, a systematic variation with pH is readily apparent in the energy of the first derivative maxima near 5480 eV, reflecting the rising edge inflection points of the XAS spectra. Systematic trends in the shape of the first derivative are also evident at 5471 eV and 5482–5490 eV. In addition, there is an increase in intensity with pH of the first derivative of the $1s \rightarrow 3d$ transition-feature at 5466 eV (Fig. 2b, inset). This same transition is also selectively affected by pH in aqueous solutions of V(III) sulfate, in which $[V(SO_4)_{1,2}]^{+,-}$ complex ions predominate [7]. However, when sulfate is present, the energy position of the maximum of absorption near 5484 eV, rather than the rising edge inflection, is shifted with pH. These differences in response illustrate the medium-specific effects that can be exploited to identify the chemical state of vanadium in complex systems, even in the absence of a distinction in oxidation-state or a large divergence in ligand environment.

The systematic nature of the pH-induced changes in the K-edge XAS of $[V(aq)]^{3+}$ is evident when the relative eV shift of the rising edge inflection is plotted against pH, shown in the inset to Fig. 2a. Because this plot had the shape of a Brønsted-acid pH titration, we attempted to fit these data with a titration model. Under conditions of, e.g. 1 M NaCl ($\mu = 1.0$) and ambient

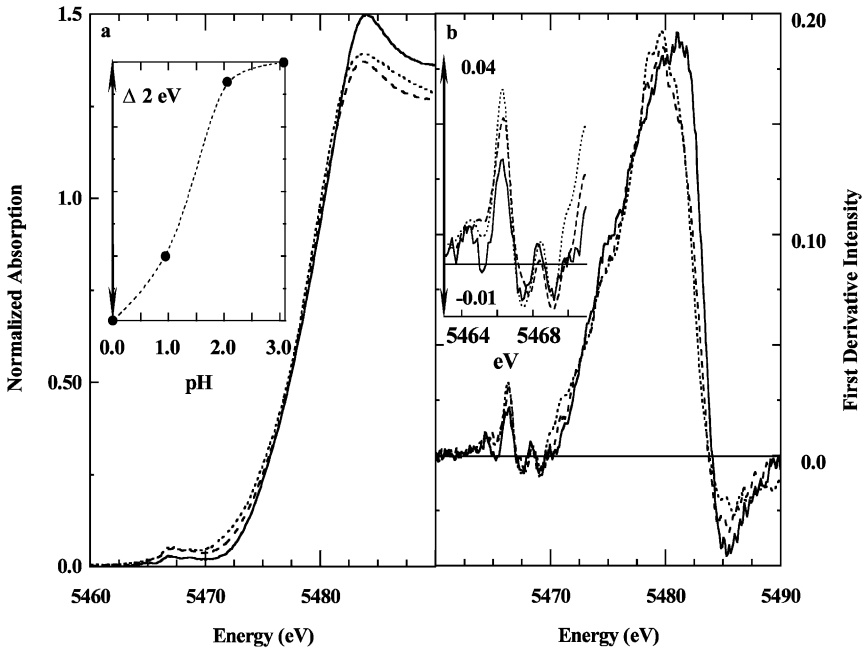

Fig. 2. (a) Vanadium K-edge XAS spectrum of 0.1 M VCl_3 in (—), pH 0.95, (---), pH 2.06, and (···), pH 3.07 aqueous solution. Note the systematic changes near 5470 eV that continue through the rising edge, and the changes in line-shape above 5484 eV. Inset a: The shift in the energy position of the rising edge inflection plotted as a function of pH. The dashed line is an arbitrary smooth curve drawn through the points. (b) The first derivatives of the XAS spectra shown in part a. Inset b: Expansion of the pre-edge portion of the XAS spectrum. Note the shift with pH of the energy position of the rising edge inflection near 5480 eV.

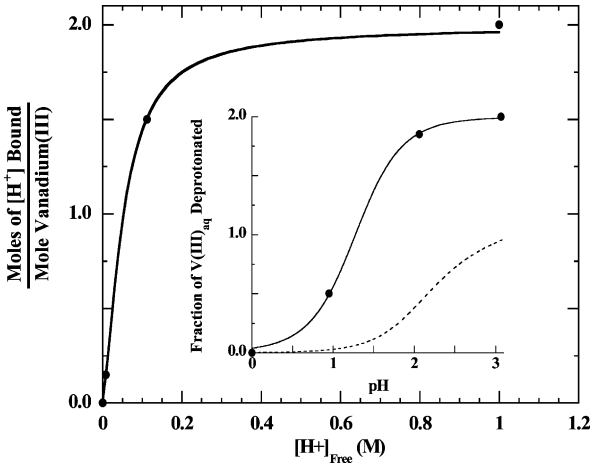

Fig. 3. (●), The shift in energy with pH of the rising edge, as shown in the Fig. 2 inset, plotted as a titration curve according to the protonation model of Reactions 1 and 2 (see text). $[H^+]_{free}$ is the concentration of free hydrogen ion in units of Molar and was measured as pH. (—), The line fitted according to the above model (see Section 2). Inset: (●), The XAS data calculated as fraction of deprotonated $V(H_2O)_6^{3+}$; (—), the fit to the data, and; (---), the line calculated from the known room temperature hydrolysis constants of V^{III} in aqueous solution, all plotted vs. pH.

temperature, $[V(H_2O)_6]^{3+}$ is known to undergo two deprotonation steps of $pK_{a1} = 2.59$ and $pK_{a2} = 3.89$ [22]. Above pH ~ 2.5, further hydrolytic reactions occur yielding oxo-bridged dimers and higher multinuclear homologues [22,23]. The XAS data of Fig. 2a, inset were analyzed in the more convenient form of the associative protonation reactions 1 and 2 below. The data were thus plotted as moles of proton bound per mole of V^{III} total, as determined by the shift in rising edge inflection energy, versus the free proton concentration measured as pH (Fig. 3). Initially, the data were modeled using the simple expression for a single equilibrium, as though, e.g., only reaction 2 (or 1) was relevant. However, a fit according to this model did not pass through the XAS data points.

$$(H_2O)_4V(OH)_2^+ + H^+ \rightleftharpoons (H_2O)_5V(OH)^{2+} \quad (1)$$

$$(H_2O)_5V(OH)^{2+} + H^+ \rightleftharpoons V(H_2O)_6^{3+} \quad (2)$$

A fit reflecting the more realistic model including both reactions 1 and 2 was constructed according to the general equation for two sequential equilibrium binding steps, as given by Klotz [17,24,25]. The fit equation used, which is valid for any pair of equilibria and which imposes no particular mechanistic bias, is described fully in Section 2. This fit represented the data extremely well ($r = 0.9997$) and is shown in Fig. 3, yielding $K_{b1} = 12 \pm 4$ M^{-1} and $K_{b2} = 29 \pm 7$ M^{-1} These results are surprising, however, because they imply a cooperative protonation reaction, in which Reaction 2 occurs more readily than Reaction 1. The corresponding pK_a values for the deprotonation of $[V(H_2O)_6]^{3+}$, obtained as the reciprocals of these K_b values, are $pK_{a1} = 1.5 \pm 0.1$ and $pK_{a2} = 1.1 \pm 0.1$, respectively. These values are very different from the pK_a values in 1 M NaCl cited above, and

likewise imply the second deprotonation (the reverse of Reaction 1) occurs with more facility than the first (the reverse of Reaction 2).

In Fig. 3 inset, the data and the fit are plotted in terms of fraction of V^{III} deprotonated as a function of pH. In the fit model, the total V^{III} fraction that can be deprotonated is 2, because according to Reactions 1 and 2 each $[V(H_2O)_6]^{3+}$ can lose a total of two protons. The fit is seen to reproduce the data very well. The dashed line in Fig. 3 inset represents the fraction of V^{III} deprotonated with pH as predicted from the known pK_a values and oligomerization constants of the $[V(H_2O)_6]^{3+}$ ion [22]. Thus at each pH the fraction of V^{III} that is deprotonated is $(2 \times [V(OH)_2]^+ + [V_2(OH)_2]^{4+} + (8/3) \times [V_3(OH)_8]^+ + 3 \times [V_4(OH)_{12}] + [VOH]^{2+})/[V]_{total}$ where water ligands are ignored. The pH-dependent concentration of each of the V^{III} hydrolytic complexes was calculated using the 'Medusa' speciation software as described in Section 2. It is clear that the predicted line does not reflect the XAS data at all. Under the experimental conditions, the ionic strength was calculated to vary over the range $\mu = 1.1$ (in the pH 0.0 solution) to $\mu = 0.80$ (in the pH 3.07 solution), neglecting H_3O^+ ion. However, deprotonation reactions of $[V(aq)]^{3+}$ are apparently not very sensitive to changes in ionic strength, in that, e.g., pK_{a1} was measured as 2.85 at $\mu = 1.0$ (NaCl) and 3.15 at $\mu = 3.0$ (NaCl) [26]. The XAS results therefore indicate that under the conditions of the experiment −10 K in frozen solution and with modestly varying ionic strength—the pK_a values for the first two deprotonations of $[V(H_2O)_6]^{3+}$ have not only departed strongly from their room temperature values, but are positively cooperative.

The usual explanation for the emergence of cooperativity in inorganic ligation reactions is that binding of the new ligands is accompanied by a decrease in the total number of ligands, leading to an increase in the per-ligand bond-strength [27,28]. In the hydrolysis of $[V(H_2O)_6]^{3+}$, this explanation is unlikely however, because there are no significant changes in the intensities or the multiplicity of the $1s \rightarrow 3d$ transitions in the pre-edge energy region of the XAS spectra (Fig. 2). The increase in intensity of the *first derivative* of the 5466 eV transition has been previously observed to accompany deprotonation of water ligands bound to V(III) in sulfate-containing solution [7], as noted above. At constant intensity, an increasing slope in the first derivative indicates a decreasing line width in the absorption feature, which may reflect an alteration in the ligand field experienced by V(III) following deprotonation of a water ligand. A site-symmetry change from octahedral coordination to, e.g. a four- or five-coordinate metal center would be accompanied by easily observable changes in the shape, multiplicity, and intensity of the $1s \rightarrow 3d$ XAS absorption features [8,29]. This is not observed in the XAS spectra of Fig. 2. The small general increase with pH evident in the absorption intensity of the pre-edge energy region is more likely due to tailing from the intensity increases occurring in the rising edge at higher energy. The first derivatives of the XAS spectra (Fig. 2b) thus maintain only the three weak transitions expected from an octahedral complex throughout the pH-series. Therefore, V^{III} apparently remains hexa-coordinate through the deprotonation process. Consequently, we suggest that the emergent cooperativity may be due to a true inversion at low temperature of the relative strengths of the two pK_a-values, implying that the free energy of reactions 1 and 2 may have a large entropic component. If so, this entropic term could involve solvent reorganization [30]. It seems likely that any such inversion would occur during the course of freezing, rather than in frozen solution. It is estimated that XAS samples freeze within about 0.1 s when immersed in a freezing pentane slush. Though rapid, this time is slow at the molecular level, where large-scale molecular motions can occur in solution within nanoseconds [31] and rotations of small ions occur in picoseconds [32,33]. In addition, proton mobility in water is rapid even at low temperature [34–36]. Therefore, we suggest that the equilibrium concentrations of deprotonated V^{III} species re-equilibrated during cooling, and the cooperative equilibria assessed by XAS are those typifying the very cold solution just prior to freezing. Cooperative deprotonation of metal ions in water solution at ambient temperatures has been observed in the hydrolysis of $[Ag(aq)]^+$ [37,38], of $[Zn(aq)]^{2+}$ [38,39], and of $[Al(aq)]^{3+}$ [27,40].

3.2. Response to pH and solvent medium

Fig. 4 shows the effect of pH on the energy position of the V^{III} XAS K-edge absorption maximum under three different solution conditions. Each line is very different. The difference in behavior with pH between V^{III}–sulfate in water and the same ions in 40% aqueous methanol can be assigned at least in part to the divergent pK_a values of sulfate in these mediums, which are 1.92 and 2.45, respectively (see Section 2). That is, because sulfate ion is more basic in methanolic solution, it is more heavily protonated at any pH than is the case in water solution, and so is less available for complex ion formation with $[V(H_2O)_6]^{3+}$. This idea is corroborated by the differential appearance of a shoulder at 5475 eV in the K-edge XAS spectrum of dissolved $V_2(SO_4)_3$ that is indicative of a V^{III}–sulfate interaction [18]. This shoulder is strongly visible in pH 1 frozen aqueous solution but becomes prominent only at pH 2 in frozen 40% aqueous methanol [7]. These data thus show that XAS spectra reflect specific solution conditions, and therefore indicate the systematics of relevant solution chemistry. Such systematic trends can be exploited to illuminate the chemical state of elements of interest

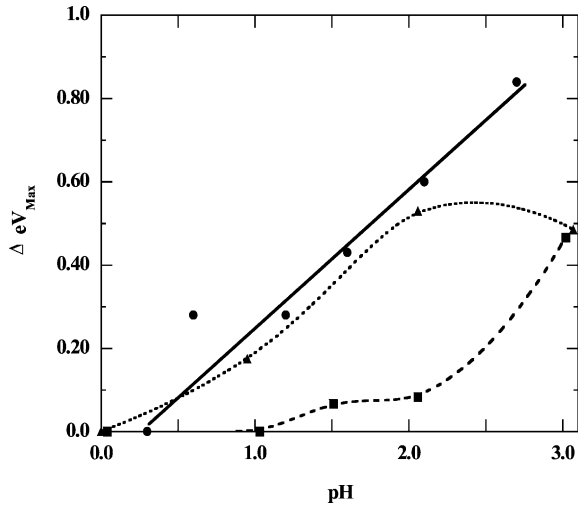

Fig. 4. The relative shift with pH in the energy of the K-edge XAS absorption maximum of aqueous V^{III} as: (●), 25 mM $V_2(SO_4)_3$ in 40% aqueous methanolic solution; (▲), 25 mM $V_2(SO_4)_3$ in aqueous solution, and; (■), 0.1 M VCl_3 in aqueous solution. The traces are arbitrary smooth lines drawn through the data points.

resident in complex milieus, even if that element exists in more than one oxidation- or ligation-state.

3.3. *A. ceratodes* blood cells and fit

Taking advantage of this sensitivity, the vanadium K-edge XAS spectra of blood cells from phlebobranch

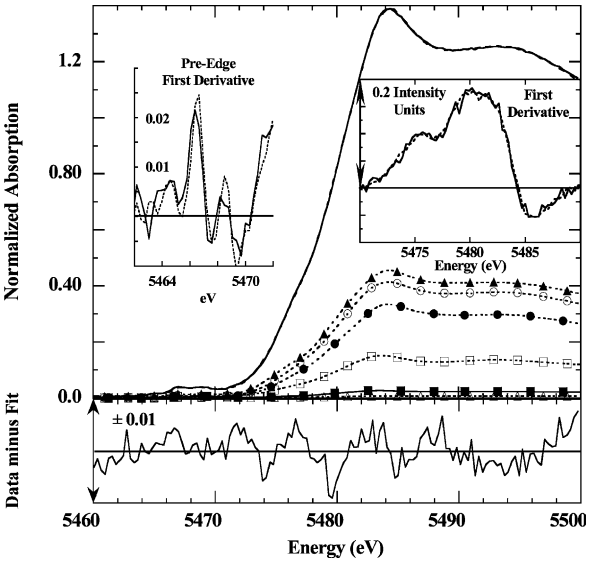

Fig. 5. Vanadium K-edge XAS spectrum of: (—), blood cells from a single specimen of *A. ceratodes* collected from Bodega Bay, CA; (---), the fit to the spectrum, and; (···), the components of the fit. The components in aqueous solution are: (▲), 25 mM $V_2(SO_4)_3$ in 448 mM sulfate, pH 1.8; (○), 50 mM $V_2(SO_4)_3$, pH 1.8; (●), 25 mM $V_2(SO_4)_3$, pH 0.04; (□), 25 mM $V_2(SO_4)_3$, pH 3.0; (■), 0.1 M $VOCl_2$ in 0.1 M HCl; (△), $K_2VO(catecholate)_2$, solid dispersed in BN. The insets show first derivatives of the vanadium K-edge XAS spectrum of: (—), the blood cell sample, and; (---), the fit to the sample. Bottom: the data minus fit residuals spectrum.

tunicates can be fit using a linear combination of XAS spectra of model complexes [7,8]. These organisms collect vanadate from sea water using their filter-feeding apparatus. The up-taken vanadium is concentrated by several orders of magnitude over the ambient sea water level, is reduced to V^{IV} and/or V^{III} and appears in at least three different types of blood cells [41–44]. In the solitary tunicate *A. ceratodes*, endemic to the temperate west coast of North America, XAS experiments have shown that more than 90% of the blood cell vanadium is retained as V^{III} ion in the presence of high sulfate concentrations and moderate to high acidity [7,10,18,45].

In Fig. 5 is shown the fit to a blood cell sample taken from a single *A. ceratodes* specimen collected from Bodega Bay, California. The components of the fit are given in the Legend of the Figure. In this fit 62.4% of the vanadium was represented by XAS models reflecting V^{III}–sulfate in a pH 1.8 solution containing excess sulfate. Nearly 11% of the endogenous vanadium was fit with the XAS of a model solution containing $V_2(SO_4)_3$ dissolved in pH 3.0 solution. The first derivatives of the data and of the fit to the data are given in the insets to the Figure. These show that the fit reproduces the energy positions of the inflection points in the data, and the positions and line-widths of the contributing transitions. This is especially evident in the pre-edge region where violation of these criteria is readily observed. At the bottom of Fig. 5, the data minus fit residuals do not exceed 1% of the intensity of the K-edge jump of the XAS spectrum.

3.4. *Vanadium in A. ceratodes and P. nigra*

In the Table 1 the specific vanadium complexes derived from the fit to the above *A. ceratodes* blood cell sample are shown. These were calculated according to the published method [7] from the distribution of V^{III} complexes in the inorganic solutions used to produce the model XAS spectra. Also shown is the average distribution of vanadium species derived from similar XAS fits [7,8], to whole blood cell packs totaling about 62 specimens of *A. ceratodes* collected from Monterey Bay, California (~210 km south of Bodega Bay, CA). These show a remarkable contrast with the vanadium content of a sample of blood cells representing 11 specimens of *P. nigra* collected from Key Largo, Florida, modeled using the same XAS fitting method. The two *A. ceratodes* samples exhibit related arrays of vanadium complexes, typifying V^{III} in aqueous solution of moderate to high acidity, and with significant concentrations of intracellular sulfate. The presence of blood cells containing a region of only moderate endogenous acidity is indicated by hydrolytic V^{III} components with oxo- and hydroxo-ligands. Relatively less of the V^{III} in blood cells of *A. ceratodes* from

Table 1
Complexes modeling vanadium in tunicate blood cells

Vanadium(III,IV) species	*P. nigra*[a] %	*A. ceratodes* (average)[b] %	*A. ceratodes*[c] %
$[V(H_2O)_6]^{3+}$	33.7	23.6	38.7
$[V(SO_4)(H_2O)_5]^{+}$	–	38.1	34.0
$[V(SO_4)_2(H_2O)_4]^{-}$	–	19.8	10.3
$[V(OH)(H_2O)_5]^{2+}$	–	3.0	2.7
$[V(SO_4)(OH)(H_2O)_4]$	–	0.7	0.4
$[V(SO_4)(OH)_2(H_2O)_3]^{-}$	–	7.7	9.9
$[V_2O(H_2O)_{10}]^{4+}$	–	0.7	0.4
$[V(catecholate)_3]^{3-}$	18.8	2.8	0.4
$[V(acetylacetonate)_3]$	14.4	–	–
VO^{2+}_{aq}	30.1	2.8	2.0
VO(bis-chelate) [d]	3.0	0.3	0.6
SO_4^{2-}/V^{III}	0.0	0.97	0.68

[a] Pooled blood cells from 11 animals collected from Key Largo, Florida, USA.
[b] Average of fits to two samples of pooled blood cells totaling 62 animals collected from Monterey Bay, California, USA.
[c] Blood cells from one animal collected from Bodega Bay, California, USA.
[d] The fits were equally good using the XAS spectra of either $K_2VO(catecholate)_2$ or $VO(acac)_2$ to model this component.

Bodega Bay appears to reside in a sulfate complex ion than is typical for this metal in specimens collected from Monterey Bay (cf. the last entry in Table 1). We intend to compare in detail the vanadium within the blood cells of *A. ceratodes* from Bodega Bay with those of the same species from Monterey Bay using XAS spectroscopy to determine the generality, if any, of the above perceptible differences in vanadium environment.

In *P. nigra*, as collected from the subtropical Florida Keys, in contrast, fits to blood cells showed that endogenous vanadium is divided into sulfate-free hexaaquaV^{III} ($\sim$34%), V^{III} in a tris-catecholate-like chelation environment ($\sim$33%), and the aqua VO^{2+} ion ($\sim$30%) [8]. Staining experiments performed on *P. mammillata* have indicated that free V^{III} ion is resident in signet-ring and other vacuolated blood cells [44,46]. The direct evidence for the endogenous tris-chelation of blood cell V^{III} in *P. nigra* was unprecedented, but confirmed inferences previously made from in vitro chromatographic separation of products from blood cell lysis [47].

The exclusive presence of the hexaaqua ion representing dissolved V(III) in *P. nigra* blood cells indicates high acidity for the endogenous V(III) environment along with the possible absence of any co-located sulfate, highlighting one of several remarkable differences between *P. nigra* and *A. ceratodes*. If sulfate is at all present in these cells, the intracellular acidity must be high enough to prevent any observable complexation of this anion to V^{III}, even on freezing. In our hands the signature of $[V(SO_4)(H_2O)_5]^{+}$ complex ion is observable at 5475 eV in the K-edge XAS spectra of frozen pH 0.0 solutions of 25 mM $V_2(SO_4)_3$, in which only 5% of the V(III) is coordinated by sulfate at room temperature. Therefore, the absence of this signal in the vanadium K-edge XAS spectra of frozen *P. nigra* blood cells implies a very low concentration, if any, of co-located sulfate.

On the other hand, the success in the fits of the tris-chelated V^{III} models indicated that a significant fraction of blood cell vanadium resides in an alternative *non-acidic* locale, because these complexes apparently are not stable in aqueous acid [48]. Tris-chelated, e.g. tunichrome, complexes of V^{III} may constitute the vanadium-containing granules detected within blood cells of *P. mammillata* [49]. Rounding out the observed differences, *P. nigra* blood cells include about an order of magnitude more aqua VO^{2+} than those of *A. ceratodes*. Thus although both *A. ceratodes* and *P. nigra* uptake, concentrate, and reduce oceanic vanadate, and deposit this metal in the same sorts of blood cells, the respective fates of blood cell vanadium are highly dissimilar.

3.5. VO^{2+} uptake into *A. ceratodes* blood cells

Finally, we report preliminary results from experiments incubating whole blood cells from *A. ceratodes* with vanadyl ion in the presence of DTT. In this experiment, DTT was added in order to prevent agglutination of blood cells. Fig. 6 shows the XAS spectra of a sample of blood cells before and after incubation with 25 mM VO^{2+} in pH 6.6 solution. Control experiments and comparative microscopic examination of control and exposed cells showed no damage to blood cells by this procedure as indicated by the absence of lysed or discolored cells and by Trypan Blue viability assay. Following incubation, blood cells were washed free of exogenous VO^{2+} by centrifugation. Examination of the pre-edge region of the Fig. 6 XAS spectrum reveals the appearance near 5469 eV of a new signal with respect to the control blood

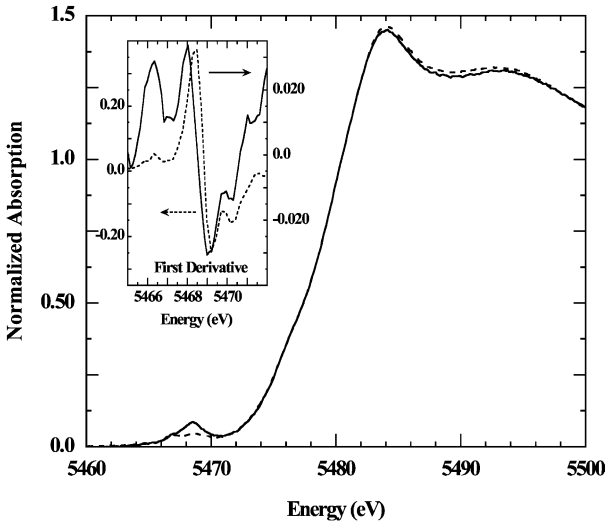

Fig. 6. Vanadium K-edge XAS spectrum of: (---), pooled blood cells from 14 specimens of *A. ceratodes* from Bodega Bay, CA, and; (—), blood cells from the same pool after incubation for 40 min at ice temperature in the presence of 25 mM each of DTT and of VO^{2+}. Inset: a comparison of the first derivatives of the pre-edge energy region of the vanadium K-edge XAS spectrum of: (—), the incubated blood cell sample, and; (···), 0.1 M $VOCl_2$ in 0.1 M HCl solution. The feature near 5466 eV reflects the continuing preponderance of V(III) [7,18] in the blood cells of the incubated sample. Note that the two inset spectra refer to different intensity axes.

cell sample. This signal indicates that vanadyl ion has been taken up into the cells during incubation. From the intensity of this signal, an estimate can be made that about 10% of the blood cell vanadium is represented by vanadyl ion. From the Table 1 this indicates an increase in the concentration of intracellular vanadyl ion by about a factor of 3.

The inset to Fig. 6 shows a comparison between the first derivative of the XAS spectrum of the new intracellular vanadyl signal and that of aquavanadyl ion in 0.1 M HCl solution. The new blood cell vanadyl ion signal exhibits a shift of about −0.35 eV relative to the energy position of the aqua-ion absorption feature. This shift is consistent with complexation of the intracellular vanadyl ion within a biological chelate. The energy shift of the pre-edge XAS absorption feature of $(VOedta)^{2-}$ is −0.4 eV relative to that of aqua VO^{2+}, for example [8]. DTT does not react with VO^{2+} in aqueous solutions below pH 7 [50]. The XAS spectrum of aqueous vanadyl ion in pH 6.6 solution (0.5 M NaCl, 25 mM sodium phosphate) with a five-fold excess of DTT is virtually identical to that of $[VO(aq)]^{2+}$ in 0.1 M HCl. Under the same solute conditions but at pH 7.9, the solution was dark green and a VO–DTT complex produced an XAS spectrum very different from that of $[VO(aq)]^{2+}$ or of the intracellular VO^{2+}. Thus the shifted vanadyl signal is not due to an adsorbed or up-taken VO^{2+}–DTT complex. This result will be reported fully elsewhere.

In conclusion, we have shown that K-edge XAS spectroscopy is sensitive to subtle aspects of solution chemistry and has significant utility in elucidating the composition of elements in complex materials. The biological chemistry of vanadium in blood cells of ascidians has turned out to be far more complex than even recently imagined [51–53]. Closely related species are now known to maintain this metal in widely divergent environments despite utilizing the same sorts of blood cells for this purpose.

Acknowledgements

This work was supported by grants NSF CHE 94-23181 and NIH RR-01209 (to KOH). XAS data were collected at SSRL, which is supported by the Department of Energy, Office of Basic Energy Sciences, Divisions of Chemical and Materials Sciences. The SSRL Biotechnology Program is supported by the National Institutes of Health, National Center for Research Resources, Biomedical Technology Program and by the Department of Energy, Office of Biological and Environmental Research.

References

[1] G.P. Huffman, N. Shah, F.E. Huggins, L.M. Stock, K. Chatterjee, J.J. Kilbane, II, M.-I.M. Chou, D.H. Buchanan, Fuel 71 (1995) 549.
[2] S.R. Wasserman, R.E. Winans, R. McBeth, Energy Fuels 10 (1996) 392.
[3] J.S. Waldo, O.C. Mullins, J.E. Penner-Hahn, S.P. Cramer, Fuel 71 (1992) 53.
[4] M.J. Morra, S.E. Fendorf, D.P. Brown, Geochim. Cosmochim. Acta 61 (1997) 683.
[5] I.J. Pickering, R.C. Prince, T. Divers, G.N. George, FEBS Lett. 441 (1998) 11.
[6] C.M.B. Henderson, G. Cressy, S.A.T. Redfern, Radiat. Phys. Chem. 45 (1995) 459.
[7] P. Frank, K.O. Hodgson, Inorg. Chem. 39 (2000) 6018.
[8] P. Frank, W.E. Robinson, K. Kustin, K.O. Hodgson, J. Inorg. Biochem. 86 (2001) 635.
[9] P. Frank, B. Hedman, R.M.K. Carlson, K.O. Hodgson, Inorg. Chem. 33 (1994) 3794.
[10] P. Frank, B. Hedman, K.O. Hodgson, Inorg. Chem. 38 (1999) 260.
[11] D.E. Ryan, K.B. Grant, K. Nakanishi, P. Frank, K.O. Hodgson, Biochemistry 35 (1996) 8651.
[12] P. Frank, R.M.K. Carlson, E.J. Carlson, K.O. Hodgson, submitted for publication, 2002.
[13] P. Frank, K.O. Hodgson, K. Kustin, W.E. Robinson, J. Biol. Chem. 38 (1998) 24498.
[14] P. Frank, R.M.K. Carlson, K.O. Hodgson, Inorg. Chem. 25 (1986) 470.
[15] R.G. Bates, M. Paabo, R.A. Robinson, J. Phys. Chem. 67 (1963) 1833.
[16] W.J. Gelsema, C.L. De Ligny, A.G. Remunse, H.A. Blijleven, Recueil 85 (1966) 647.
[17] I.M. Klotz, D.L. Hunston, J. Biol. Chem. 259 (1984) 10060.

[18] P. Frank, K. Kustin, W.E. Robinson, L. Linebaugh, K.O. Hodgson, Inorg. Chem. 34 (1995) 5942.
[19] S.P. Cramer, K.O. Hodgson, Prog. Inorg. Chem. 25 (1979) 1.
[20] W.H. Press, B.P. Flannery, S.A. Teukolsky, W.T. Vetterling, Numerical Recipes, Cambridge University Press, Cambridge, 1989, p. 523.
[21] I.M. Klotz, Accts. Chem. Res. 7 (1974) 162.
[22] R. Meier, M. Bodin, S. Mitzenheim, K. Kanamori, in: H. Sigel, A. Sigel (Eds.), Metal Ions in Biological Systems: Vanadium and Its Rôle for Life, vol. 31, Marcel Dekker, New York, 1995, p. 45.
[23] L. Pajdowski, J. Inorg. Nucl. Chem. 28 (1966) 433.
[24] I.M. Klotz, D.L. Hunston, Arch. Biochem. Biophys. 193 (1979) 314.
[25] A. Ben-Naim, Curr. Top. Solution Chem. 2 (1997) 95.
[26] L. Pajdowski, in: B. Jezowska-Trzebiatowska (Ed.), Theory and Structure of Complex Compounds, Macmillan, New York, 1964, p. 589.
[27] R.B. Martin, in: H. Sigel, A. Sigel (Eds.), Metal Ions in Biological Systems: Aluminum and Its Role in Biology, vol. 24, Marcel Dekker, Inc, New York, 1988, p. 1.
[28] R.B. Martin, Comments Inorg. Chem. 18 (1996) 249.
[29] T.E. Westre, P. Kennepohl, J.G. DeWitt, B. Hedman, K.O. Hodgson, E.I. Solomon, J. Am. Chem. Soc. 119 (1997) 6297.
[30] D.L. Sackett, H.A. Saroff, FEBS Lett. 397 (1996) 1.
[31] O. Tcherkasskaya, O.B. Ptitsyn, J.R. Knutson, Biochemistry 39 (2000) 1879.
[32] F.L. Baker, W.M. Smith, Can. J. Chem. 48 (1970) 3100.
[33] M. Perrot, F. Guillaume, W.G. Rothschild, J. Phys. Chem. 87 (1983) 5193.
[34] B.E. Conway, J.O.M. Bockris, J. Chem. Phys. 28 (1958) 354.
[35] H. Engelhardt, B. Bullemer, N. Riehl, Phys. Ice, Proc. Int. Symp., 3rd, Tech. Hochsch. Muenchen, Munich, Ger., 1968, p 430.
[36] T.H. Huang, R.A. Davis, U. Frese, U. Stimming, J. Phys. Chem. 92 (1988) 6874.
[37] E. Carriere, H. Guiter, Bull. Soc. Chim. Fr. (1947) 267.
[38] C.F. Baes, R.E. Mesmer, The Hydrolysis of Cations, Wiley-Interscience, New York, 1976.
[39] D. Ferri, F. Salvatore, Ann. Chim. 78 (1988) 83.
[40] R.B. Martin, J. Inorg. Biochem. 44 (1991) 141.
[41] E.M. Oltz, S. Pollack, T. Delohery, M.J. Smith, M. Ojika, S. Lee, K. Kustin, K. Nakanishi, Experientia 45 (1989) 186.
[42] H. Michibata, Y. Iwata, J. Hirata, J. Exp. Zool. 257 (1991) 306.
[43] G.W. Nette, S. Scippa, M. de Vincentiis, Ivert. Reprod. Dev. 34 (1998) 195.
[44] G. Nette, S. Scippa, M. Genovese, M. de Vincentiis, Comp. Biochem. Physiol. C122 (1999) 231.
[45] T.D. Tullius, W.O. Gillum, R.M.K. Carlson, K.O. Hodgson, J. Am. Chem. Soc. 102 (1980) 5670.
[46] S.W. Taylor, B. Kammerer, E. Bayer, Chem. Rev. 97 (1997) 333.
[47] E.M. Oltz, R.C. Bruening, M.J. Smith, K. Kustin, K. Nakanishi, J. Am. Chem. Soc. 110 (1988) 6162.
[48] E. Kime-Hunt, K. Spartalian, S. Holmes, M. Mohan, C.J. Carrano, J. Inorg. Biochem. 41 (1991) 125.
[49] S. Scippa, K. Zierold, M. de Vincentiis, J. Submicrosc. Cytol. Pathol. 20 (1988) 719.
[50] P.A.M. Williams, D.A. Barrio, S.B. Etcheverry, J. Inorg. Biochem. 75 (1999) 99.
[51] H. Michibata, Adv. Biophys. 29 (1993) 105.
[52] M.J. Smith, D.E. Ryan, K. Nakanishi, P. Frank, K.O. Hodgson, in: H. Sigel, A. Sigel (Eds.), Metal Ions in Biological Systems: Vanadium and Its Rôle for Life, vol. 31, Marcel Dekker, New York, 1995, p. 423.
[53] H. Michibata, T. Uyama, K. Kanamori, ACS Symp. Ser. 711 (Vanadium Compounds) (1998) 248.